2014

Orbital Solutions and Absolute Elements of the Short-Period Eclipsing Binary ES Librae

Nicole E. Cabrera
Georgia State University

James R. Sowell
Georgia Institute of Technology

Richard M. Williamon
Emory University

Thomas F. Collins
Clemson University

Francis C. Fekel
Tennessee State University

See next page for additional authors

Recommended Citation

Nicole E. Cabrera et al 2014 PASP 126 121

Authors

Nicole E. Cabrera, James R. Sowell, Richard M. Williamon, Thomas F. Collins, Francis C. Fekel, Michael H. Williamson, and Matthew W. Muterspaugh

Publications of the Astronomical Society of the Pacific, **126**:121–132, 2014 February

Orbital Solutions and Absolute Elements of the Short-Period Eclipsing Binary ES Librae

Nicole E. Cabrera,[1,2] James R. Sowell,[2] Richard M. Williamon,[3] Thomas F. Collins,[4] Francis C. Fekel,[5] Michael H. Williamson,[5] and Matthew W. Muterspaugh[5]

Received 2013 October 09; accepted 2013 December 21; published 2014 February 10

ABSTRACT. We have obtained new differential UBV photoelectric photometry and radial velocities of both components of the short-period eclipsing binary ES Lib. The system has a circular orbit with a period of 0.883040928 days and is seen at an inclination of 70.1°. With the Wilson-Devinney analysis program, we obtained a simultaneous solution of our photometric and spectroscopic observations that resulted in masses of $M_1 = 2.30 \pm 0.03\ M_\odot$ and $M_2 = 0.97 \pm 0.01\ M_\odot$ and the equal-volume radii of $R_1 = 2.69 \pm 0.02\ R_\odot$ and $R_2 = 1.83 \pm 0.01\ R_\odot$ for the primary and secondary, respectively. The secondary is oversized and overluminous for its mass. The effective temperatures of the primary and secondary are 8500 K (fixed) and 5774 ± 57 K, respectively. Despite the very large temperature difference, our photometric and spectroscopic data indicate that ES Lib is not semidetached but rather require it to be in an overcontact state, where both components exceed their critical Roche lobes. Given its nonthermal equilibrium state, if the overcontact solution correctly characterizes the system, the change from being semidetached to overcontact may have occurred recently. While the asymmetry of the light curves can be modeled well with a large, hot starspot or a large, cool one on the secondary component, we prefer the latter interpretation because cool spots are a typical feature on many contact binaries.

Online material: extended tables, color figures

1. INTRODUCTION

The light variability of ES Lib [HD 135681, BD $-$ 12°4227, HIP 74765, SAO 159146; $\alpha = 15^h16^m48.^s40$, $\delta = -13°02'20.''7(2000)$] was discovered by Strohmeier et al. (1964) on sky patrol plates of the Bamberg Southern Station. Their first determination of the period was 0.49414 days, followed by a revised but still preliminary value of 0.612077 days (Strohmeier 1966). Shortly thereafter, Bartolini et al. (1968) obtained a series of spectroscopic observations at Asiago Observatory that did not agree with either preliminary period, and so they also acquired a new set of photometric observations, which they used to correct the period to 0.883036 days. Later, Bartolini et al. (1973) reanalyzed that data, which consisted of 520 single-band V photoelectric values as well as 42 radial velocity (RV) measurements of the primary component. They assumed the system was detached and obtained a light-curve solution, but also allowed for the possibility that the primary filled its Roche lobe. Giuricin et al. (1981) used the modeling program of Wood (1972) to reanalyze the Bartolini et al. (1973) data. They adopted a mass ratio of 0.4, which turns out to be very close to our computed value of 0.423. Their results indicated the primary had filled its Roche lobe, but the secondary was detached or in a broken-contact state. Milano et al. (1989) used the Wilson-Devinney (WD) program (Wilson & Devinney 1971) in their "direct seach" mode on the Bartolini et al. (1973) data. They, too, concluded the primary was filling its Roche lobe but that the secondary was not. Radial velocities were obtained by Coughlin (2007), but these cover just a small portion of the orbit, from about photometric phases 0.25 to 0.30, near minimum velocity of the primary.

Recognizing ES Lib was in need of both more photometric and spectroscopic measurements, we obtained 344 data points in each of the UBV bands. Likewise, new radial velocities were acquired during 2011 and 2012. These data include many velocity measurements of the secondary component near the two quadratures. We significantly improved the period via a least-squares fit to times-of-minima values and then analyzed our photometric and spectroscopic data simultaneously with the WD software. As a result, we have obtained an excellent solution of the orbital elements and absolute dimensions. The best

[1] Current address: Department of Physics and Astronomy, Georgia State University, Atlanta, GA 30303.

[2] School of Physics, Georgia Institute of Technology, Atlanta, GA 30332; jim.sowell@physics.gatech.edu.

[3] Department of Physics, Emory University, Atlanta, GA 30322; rwilliamon@physics.emory.edu.

[4] Department of Physics and Astronomy, Clemson University, Clemson, SC 29631.

[5] Center of Excellence in Information Systems, Tennessee State University, Nashville, TN 37209; fekel@evans.tsuniv.edu, michael.h.williamson@gmail.com, matthew1@coe.tsuniv.edu.

fit to our data requires that the system is in an overcontact state—not semidetached or detached. In addition, our preferred solution indicates the secondary had a large cool starspot during the time of our photometric observations. Our reanalysis of the Bartolini et al. (1973) photometry also results in the system being in an overcontact state.

2. OBSERVATIONS AND REDUCTIONS

2.1. Photometric

Most of our photometric observations of ES Lib were obtained by T. F. Collins with the 30 inch Cassegrain reflector at the Rosemary Hill Observatory of the University of Florida on thirteen nights during 1969 and 1970. These observations were collected with an unrefrigerated EMI 6256B photomultiplier tube, recorded with a Honeywell strip-chart recorder, and read with a 5 s timing accuracy. Observations in yellow light were made through a Corning 3384 filter, while the blue were taken through a combined Corning 5030 and Schott GG-13 filter set, and the ultraviolet measurements used a Corning 9863 filter. The effective wavelengths of the filter-photocell combinations closely approximate those of the Johnson & Morgan (1953) standard UBV system.

A night of photometric observations was added in 1983 specifically to obtain an accurate time of minimum and to calibrate the comparison and check stars used by Collins. These UBV data were obtained by R. M. Williamon using the 36 inch reflector at the Fernbank Science Center Observatory. Standard UBV filters similar to those used by Collins were combined with an unrefrigerated EMI 6256s photomultiplier to again closely approximate the effective wavelength of the Johnson-Morgan passband system. The Fernbank observations were recorded with a Honeywell strip-chart recorder, and deflections were read with a 5 s timing accuracy. All observations of ES Lib were made differentially with respect to the comparison star HD 135637 (SAO 159140), and these were corrected for atmospheric extinction by means of nightly coefficients determined from the comparison star via the technique of Hardie (1962). The Heliocentric Julian Dates and differential magnitudes for all of the observations are given in Table 1. Measurements of the check star HD 136276 (SAO 159180) were obtained on several nights with no indication of any variability of the comparison star.

2.2. Spectroscopic

From 2011 January through 2012 May we acquired 176 usable spectra with the Tennessee State University 2 m automatic spectroscopic telescope and a fiber-fed echelle spectrograph that are at the Fairborn Observatory in Arizona. For the first 6 months of observation the detector was a 2048×4096 SITe ST-002A CCD (Eaton & Williamson 2007). The resulting echelle spectrograms have 21 orders that cover the wavelength range 4920–7100 Å. In the summer of 2011 the SITe CCD detector and dewar were replaced by a Fairchild 486 CCD. That new detector has an array of 4096×4096 15 μm pixels and was housed in a new dewar. These most recent echelle spectrograms have 48 orders and cover the wavelength range 3800–8260 Å. Given the very broad stellar lines of both the primary and secondary, we used the largest diameter fiber, which produced a spectral resolution of 0.4 Å and resulted in typical signal-to-noise ratios of about 150 at 6000 Å. See Fekel et al. (2013) for a more extensive description of the recent system upgrades.

Fekel et al. (2009) have provided a general description of the velocity measurement for the Fairborn Observatory echelle spectra. In the case of ES Lib, we needed to use different line lists for the two components. Because of its early spectral type, A3 IV (Houk & Smith-Moore 1988), we adopted a line list for the primary that consists mostly of singly-ionized elements such as Fe II, Si II, Ti II, and Cr II, which are prominent features in A and early-F stars. The secondary, according to photometric results (Bartolini et al. 1973; Giuricin et al. 1981), is a G or K star. Thus, we used our line list for solar-type stars to determine its velocities. In addition, because the lines of both components have large rotational velocities, we fitted the lines with rotationally broadened profiles (Lacy & Fekel 2011), with both the broadening and depth being free parameters.

The new velocities are on an absolute scale. Our unpublished measurements of several IAU solar-type velocity standards indicate that the Fairborn Observatory velocities from the SITe CCD have a small zero-point offset of $-0.3\ \mathrm{km\,s^{-1}}$ relative to the velocities of Scarfe (2010). Thus, we have added

TABLE 1

ES Lib Photometric Observations

Helio. Julian Date (HJD −2,400,000)	ΔV (mag)	Helio. Julian Date (HJD −2,400,000)	ΔB (mag)	Helio. Julian Date (HJD −2,400,000)	ΔU (mag)
40,347.78721	−0.905	40,347.78773	−0.956	40,347.78819	−0.909
40,347.79495	−0.910	40,347.79557	−0.957	40,347.79618	−0.913
40,347.80317	−0.916	40,347.80374	−0.970	40,347.80435	−0.916
40,347.81167	−0.895	40,347.81227	−0.954	40,347.81288	−0.915
40,347.82044	−0.902	40,347.82107	−0.945	40,347.82171	−0.902

Note.—Table 1 is presented in its entirety in the electronic edition of the *PASP*. A portion is shown here for guidance regarding its form and content.

TABLE 2
ES LIB RADIAL VELOCITIES

Helio. Julian Date (HJD −2,400,000)	Phase[a]	RV_1 (km s^{-1})	$(O-C)_1$ (km s^{-1})	RV_2 (km s^{-1})	$(O-C)_2$ (km s^{-1})
55,990.9241	0.071	86.0	0.5	−188.0	6.2
55,997.8839	0.952	85.0	−5.4	−198.0	7.9
56,003.8364	0.693	−24.0	5.6	…	…
56,014.9454	0.274	−23.0	−11.7	…	…
56,022.8020	0.171	51.0	4.8	…	…

NOTE.—Table 2 is presented in its entirety in the electronic edition of the *PASP*. A portion is shown here for guidance regarding its form and content.

[a] Phases are from the combined spectroscopic solution of Table 3, where zero phase is a time of maximum velocity of the primary.

$0.3\ \mathrm{km\,s^{-1}}$ to those Fairborn velocities. A similar analysis for the Fairchild CCD results shows an offset of $-0.6\ \mathrm{km\,s^{-1}}$, so $0.6\ \mathrm{km\,s^{-1}}$ has been added to each of those velocities. Table 2 gives the Heliocentric Julian Dates of mid-observation and the primary and secondary radial velocities for those dates. Also given in that table are the fractional phases of the observations, which have been computed from a time of maximum positive velocity of the primary, and the residuals to the orbit. The listed phases and residuals are from the final spectroscopic solution discussed in § 3.

3. SPECTROSCOPIC ORBIT

Circular orbits for ES Lib were determined with the computer programs SB1C and SB2C (D. Barlow 1998, private communication), which use differential corrections to compute improved orbital elements. From our spectra we measured 176 radial velocities of the primary and 38 of the secondary. We initially determined separate orbits for the two components with the orbital period fixed at our newly computed photometric value (§ 4). From the variances of the two solutions, the velocities of the primary and secondary were given weights of 0.7 and 1.0, respectively. The weights of the primary velocities are smaller because, although the average line depth of that component is greater, its lines are 50% broader and sometimes asymmetric, making velocities of the primary less precise.

We note that the center-of-mass velocities of the two orbits differ by $5\ \mathrm{km\,s^{-1}}$. This difference at least partially results from the velocity uncertainties caused by the very broad-lined nature of the two components and perhaps partly from the use of two very different line lists. Table 3 gives the orbital elements and additional quantities derived from the two solutions.

Despite the moderate center-of-mass velocity difference between the two components, we computed a combined orbital solution for the Fairborn Observatory data. Compared with the single component solutions, the semiamplitudes of both components in the combined solution have increased, but those increases are $\lesssim 0.2\%$ and significantly less than the 1σ uncertainties. The orbital elements and derived quantities for the combined solution are also presented in Table 3. For a circular orbit the element T, a time of periastron passage, is undefined.

TABLE 3
SPECTROSCOPIC ORBITAL ELEMENTS

Parameter	Component 1	Component 2	Combined
P[a] (days)	0.88304093 (adopted)	0.88304093 (adopted)	0.88304093 (adopted)
T_0[b] (HJD)	2455822.1997 ± 0.0010	2455822.6461 ± 0.0015	2455822.2007 ± 0.0009
γ (km s^{-1})	1.35 ± 0.49	6.56 ± 0.89	2.43 ± 0.44
K_1 (km s^{-1})	91.87 ± 0.67	…	91.99 ± 0.72
K_2 (km s^{-1})	…	217.48 ± 0.94	217.93 ± 1.00
e	0.0 (adopted)	0.0 (adopted)	0.0 (adopted)
$a_1 \sin i$ (10^6 km)	1.1156 ± 0.0082	…	1.1170 ± 0.0087
$a_2 \sin i$ (10^6 km)	…	2.641 ± 0.011	2.6462 ± 0.0121
$m_1 \sin^3 i$ ($M_\odot$)	…	…	1.915 ± 0.023
$m_2 \sin^3 i$ ($M_\odot$)	…	…	0.808 ± 0.011
m_2/m_1	…	…	0.4221 ± 0.0038
Std error[c] (km s^{-1})	6.2	4.9	5.5

NOTE.—Solution computed from spectroscopic data alone.

[a] Photometric period.

[b] Time of maximum velocity.

[c] Standard error of unit weight observation.

So, as recommended by Batten et al. (1989), T_0, a time of maximum velocity, is used instead. Thus, zero phase of our double-lined spectroscopic orbit is at the time of the maximum velocity of the primary, and that phase is 0.25 earlier than the zero phase computed from the primary eclipse ephemeris. We also obtained an orbital solution of the combined primary and secondary velocities with the period as a free parameter. The resulting period is 0.8830363 ± 0.0000059 days, which differs by less than 1σ from the more accurate photometric period computed in § 4.

4. TIMES OF MINIMA AND ECLIPSE EPHEMERIDES

Comparing the values of the orbital period from previous observational programs with the initial analysis of our UBV data and with the period based on the radial velocity measurements, it was immediately apparent that the period needed revision, given the ~40 yr range of the observations. We obtained 11 photoelectric times-of-minima (TOM) measurements from the "O-C Gateway" Website (B.R.N.O. Project 2011). We supplemented this set with two measurements based on our photometry. These two values were obtained by applying our preliminary WD solution to the two individual nights and allowing the epoch parameter to vary. The two results are each based on a simultaneous solution of the UBV data. All of the utilized TOM measurements are listed in Table 4.

The $O - C$ plot (see Fig. 1) showed that the 0.8830356 day period of Bartolini et al. (1973) needed to be revised. Because the TOM measurements were well fit by a linear regression, the only action required was to refine the period so that the slope of the line would be horizontal. Figure 2 shows the least-squares fit through the TOM measurements that results from the improved period and epoch of 0.883040969 days and HJD 2,440,329.46785, respectively. As we progressed with

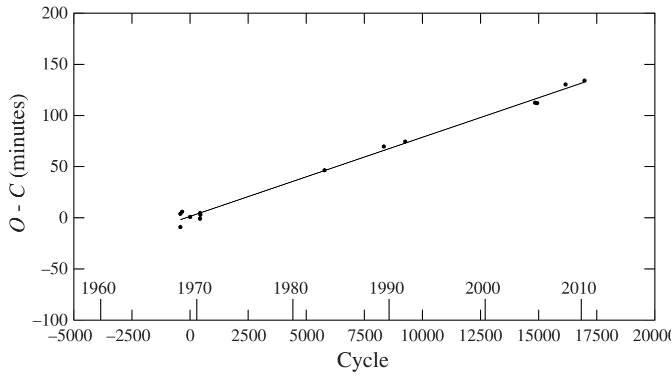

FIG. 1.—Data points are primary eclipse times-of-minima observations. The values are the photoelectric, high-precision measurements listed in Table 4. The sizes of the data points are larger than the reported error bars. The ephemeris used is HJD $2,440,329.4669 + 0.8830356E$ days from Bartolini et al. (1973). The line is a least-squares fit to the data.

our analysis, we replaced the epoch with the first of our two times of minima. Then we allowed the WD program to vary it and the period, but only small adjustments resulted.

For our improved photometric ephemeris, we define phase 0.0 as the time of mid-primary eclipse:

$$\text{Minimum Light(HJD)} = 2,440,712.70777 \pm 0.00042 + 0.883040928 \pm 0.000000056E \text{ days.}$$

5. COMBINED LIGHT AND VELOCITY SOLUTION

Light and velocity curve solutions were computed with the 2013 version of the Wilson-Devinney program. The program's physical model is described in detail in Wilson & Devinney (1971), Wilson (1979, 1990, 2012a, 2012b), Van Hamme & Wilson (2007), and Wilson et al. (2010). Our UBV photometry

TABLE 4
TIMES OF PRIMARY MINIMA

HJD—2,400,000.0	Mode	References
39,966.533	pe	1
39,967.425	pe	2
40,028.356	pe	3
40,329.4675	pe	1
40,707.4055	pe	1
40,712.70756	UBV	4
40,720.65373	UBV	4
47,690.500	ccd	5
48,500.247	V	6
53,439.9745	ccd	7
53,517.6814	ccd	8
54,598.5296	R	9
55,319.0892	I_c	10

REFERENCES.—(1) Bartolini 1970; (2) Bartolini et al. 1968; (3) Knigge & Koehler 1969; (4) This paper; (5) Diethelm 1990; (6) ESA 1997; (7) Krajci 2006; (8) Ogloza et al. 2008; (9) Brat et al. 2008; (10) Nagai 2011.

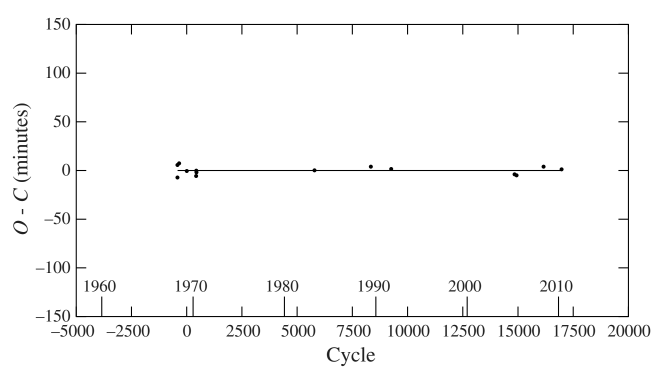

FIG. 2.—Residuals for the same data set as in Fig. 1 but now with the improved ephemeris based on the least-squares fit to the times-of-minima observations. This result was subsequently refined by the Wilson–Devinney program, and that final ephemeris is Minimum $\text{Light(HJD)} = 2,440,712.70777 \pm 0.00042 + 0.883040928 \pm 0.000000056E$ days. The horizontal line is the least-squares fit to the data.

TABLE 5
MEASUREMENT CHARACTERISTICS

Curve	Data Points	Normal Mag	σ[a]
V	344	−0.930	0.012
B	344	−0.980	0.014
U	344	−0.940	0.014
RV_1	176	…	6.9 km s^{-1}
RV_2	38	…	6.9 km s^{-1}

[a] For the light curves, in units of total light at phase 0.25.

and double-lined radial velocity data were solved simultaneously to improve parameter consistency (Wilson 1979; Van Hamme & Wilson 1984, 1985). Each observation in each data set was assigned a weight of one. Curve-dependent weights were computed from the standard deviations that are listed in Table 5. Light level-dependent weights were applied inversely proportional to the square root of the light level. Gravity darkening (g) and bolometric albedo (A) coefficients were fixed at radiative-envelope, canonical values from Lucy (1967) for the primary, whereas the secondary was assigned those for convective envelopes. A square-root limb-darkening law with coefficients x, y from Van Hamme (1993) was adopted, and the detailed reflection treatment of Wilson (1990) was used with two reflections. We utilized the improved atmosphere model option. Values of these nonvarying parameters are listed in Table 6.

Houk & Smith-Moore (1988) classified ES Lib as an A3 IV star, while Abt produced two independent classifications of A2 V (Abt 2004) and A3 III (Abt 2009). However, Hβ photometry from Wolf & Kern (1983) suggests a slightly later spectral class of about A5. Our $B - V \sim 0.20$ and $b - y = 0.145$ from Wolf & Kern (1983) indicate an even later A7 or A8 star (see Gray et al. 2001). For the secondary, the photometric results of Bartolini et al. (1973) and Giuricin et al. (1981) place it as a G or K star. These very approximate spectral classes were confirmed by an inspection of our spectroscopic data. We set the primary's temperature at that of an A5 star, 8500 K, and held it fixed. After we obtained our WD solution, we adjusted the primary's temperature by ± 500 K and obtained two additional solutions.

TABLE 6
NONVARYING WD PARAMETERS

Parameter	Symbol	Value
Rotation/Orbit Ratio	F_1, F_2	1.00, 1.00
Albedo (bolo)	A_1, A_2	1.00, 0.50
Gravity Darkening	g_1, g_2	1.00, 0.32
Limb Darkening (bolo)	x_1, y_1	+0.356, +0.348
Limb Darkening (bolo)	x_2, y_2	+0.189, +0.527
Limb Darkening (V)	x_1, y_1	+0.077, +0.690
Limb Darkening (V)	x_2, y_2	+0.254, +0.584
Limb Darkening (B)	x_1, y_1	+0.132, +0.753
Limb Darkening (B)	x_2, y_2	+0.534, +0.350
Limb Darkening (U)	x_1, y_1	+0.134, +0.630
Limb Darkening (U)	x_2, y_2	+0.705, +0.200

For the three temperatures, the 8500 K solution had the smallest sum of the squares of the residuals. Allowing for the unknown uncertainty in temperature and the temperature range associated with our $B - V$ error bar (see Allen 2000), we estimate the absolute uncertainty in T_1 to be ± 200 K. Consequently, the derived T_2 value would have a similar error, although we quote in Table 7 the much smaller relative error between the components that is computed by the WD software.

We began with Mode 2 of the WD program since this allowed each surface potential to be independently adjusted. However, this mode consistently indicated that both the primary and the secondary stars were larger in size than their Roche lobes. Therefore, we utilized the two semidetached modes for trials. First, we obtained solutions using the primary-filling-lobe situation (Mode 4), and then later we used the secondary-filling assumption for Algol-type binaries, Mode 5. For both, we tried numerous scenarios with and without a cool spot. In all of the simulation results for these two types of semidetached systems, the WD solutions consistently forced the adjustable surface potential to exceed the critical Roche lobe. Thus, we switched to Mode 3, which is the overcontact scenario for W Ursa Majoris (W UMa) stars. This mode has the surfaces in physical contact but allows the surface temperatures to be different. We assumed the orbit is circular, and our analysis provided no evidence for a third star in the system.

To improve the fit of the theoretical light curves to the UBV measurements for the overcontact configuration, a single spot was necessary. Successful simulations with convergence and excellent fits to all of the data were found for (1) a cool spot on the hotter primary, (2) a hot spot on the cooler secondary, and (3) a cool spot on the secondary. A cool starspot to fit the light curve of a W UMa star was first proposed by Binnendijk (1960) for AH Vir. Cool spots as well as chromospheric activity are often found on rapidly rotating, convective outer atmosphere, late-type stars, including W UMa type binaries (e.g., Niarchos et al. 1997; Hendry & Mochnacki 2000; Barnes et al. 2004). Of the above three solutions, we have rejected the one with the cool spot on the 8500 K primary since that star has a radiative outer atmosphere. We initially retained the remaining two solutions, the one with the hot spot on the secondary and the other with the cool spot on the secondary. The resulting orbital elements and stellar parameters of those two solutions are given in Table 7.

In comparing the two solutions, when the cool spot is changed to a hot spot, the temperature of the secondary's unspotted surface is reduced by 200 K, and the spot moves to the opposite side of the star and now has a greatly increased temperature. Of these two solutions, we have deemed the hot spot solution the less likely because we found no evidence of such a spot in our spectra and no significant evidence for third light in the system. We also note that a hot spot due to mass transfer would be at odds with an overcontact configuration. Thus, in what follows we will discuss results from the solution with the cool starspot on the secondary.

TABLE 7
Light and Velocity Curve Results

Parameter	Symbol	Cool Spot Solution	Hot Spot Solution
Period (days)	P	$0.883040928 \pm 0.000000056$	$0.883041011 \pm 0.000000053$
Epoch (HJD)	T_0	$2440712.70777 \pm 0.00042$	$2440712.70632 \pm 0.00032$
Eccentricity	e	0.0[b]	0.0[b]
Systemic velocity (km s^{-1})	γ	2.18 ± 0.44	2.18 ± 43
Semimajor axis ($R_\odot$)	a	5.753 ± 0.025	5.769 ± 0.025
Inclination (deg)	i	70.08 ± 0.15	69.61 ± 0.15
Mass ratio	M_2/M_1	0.4233 ± 0.0031	0.4226 ± 0.0035
Surface potential	Ω_1	2.6842 ± 0.0086	2.7008 ± 0.0088
Surface potential	Ω_2	2.6842[c]	2.7008[c]
Temperature (K)	T_1	8500[b]	8500[b]
Temperature (K)	T_2	5774 ± 57	5574 ± 53
Luminosity ratio[a]	$L_1/(L_1+L_2)_V$	0.9065 ± 0.0038	0.9194 ± 0.0039
Luminosity ratio[a]	$L_1/(L_1+L_2)_B$	0.9417 ± 0.0039	0.9524 ± 0.0041
Luminosity ratio[a]	$L_1/(L_1+L_2)_U$	0.9440 ± 0.0040	0.9569 ± 0.0041
Spot Parameters:			
Latitude (deg)		0.0[b]	0.0[b]
Longitude (deg)		256.2 ± 7.7	76.3 ± 4.0
Radius (deg)		40.5 ± 11.2	20.1 ± 10.2
Temperature Factor		0.884 ± 0.131	1.312 ± 0.237
Auxiliary Quantities:			
RV semiamplitude (km s^{-1})	K_1	92.1 ± 0.3	92.3 ± 0.3
RV semiamplitude (km s^{-1})	K_2	217.7 ± 0.3	217.4 ± 0.3
Distance (pc)	d	194 ± 9	191 ± 9

Note. —Wilson-Devinney simultaneous solution, including proximity and eclipse effects, of the light and velocity data.
[a] Normalized at phase 0.25 for the cool spot solution and at 0.75 for the hot spot one.
[b] Adopted value, see text.
[c] Set equal to the surface potential of the primary.

We note that for the cool spot configuration the spot is centered on the equator (i.e., 0°) and at surface longitude 256.2°, which corresponds to phase 0.712 in the light curves. The spot's angular radius is 40.5°, and its temperature factor of 0.884 equates to 5104 K versus the average surface temperature of 5774 K.

Figure 3 shows the observed measurements along with the light curves computed in each bandpass from our orbital elements, and Figure 4 plots the UBV residuals. The individual radial velocities are compared with the computed curves in Figure 5. For the primary component, all phases of the radial velocity curve are well covered including the region around primary eclipse. Because the eclipses are partial, the Rossiter effect (Rossiter 1924) is greatly diminished, although we note that the average line profile of the primary is very asymmetric before and after primary eclipse. These asymmetries produce the systematic velocity residuals that are apparent around zero phase (Fig. 6). The systematic shift of the secondary velocity residuals seen in Figure 6 results from the simultaneous solution of the radial velocities of the primary and secondary, which have different systemic velocities. As noted in § 3, the changes of the resulting semiamplitudes in the joint double-lined solution, compared to the single-lined solutions, are less than their 1σ uncertainties.

The two components have expected absolute dimensions for the parameter values and constraints used. The masses are $M_1 = 2.30 \pm 0.03\ M_\odot$ and $M_2 = 0.97 \pm 0.01\ M_\odot$, and the equal-volume radii are $R_1 = 2.69 \pm 0.02\ R_\odot$ and

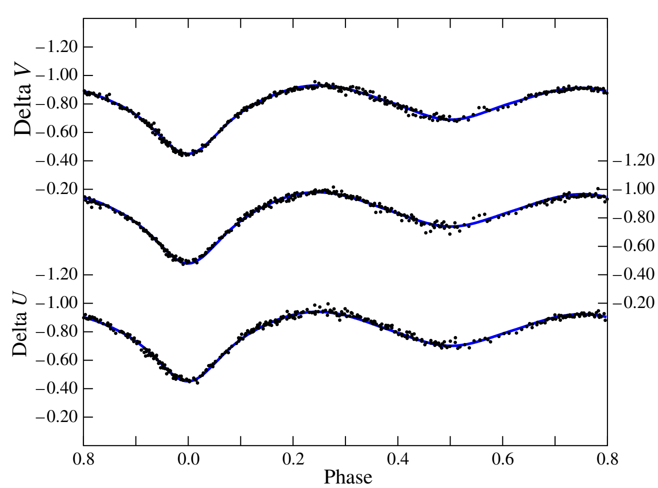

Fig. 3.—Our differential UBV magnitudes of ES Lib plotted with the Wilson–Devinney solution curves. The system is an overcontact binary, and a large, cool spot is on the secondary, which depresses the light curve in the 0.712 phase region. See the electronic edition of the *PASP* for a color version of this figure.

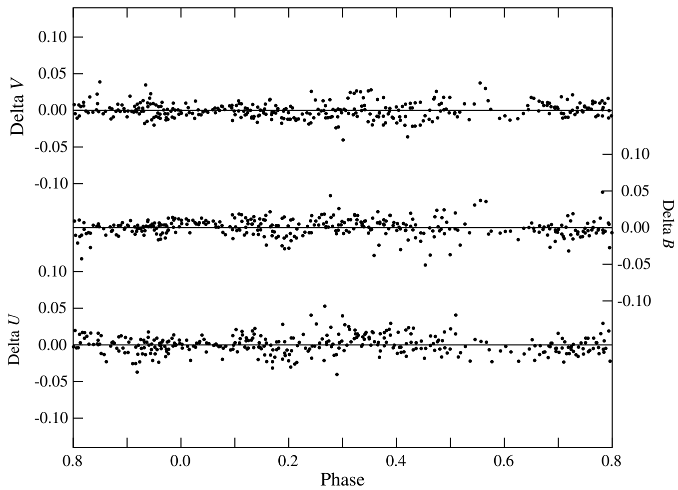

FIG. 4.—Residuals between the theoretical curves and the UBV data of Fig. 3.

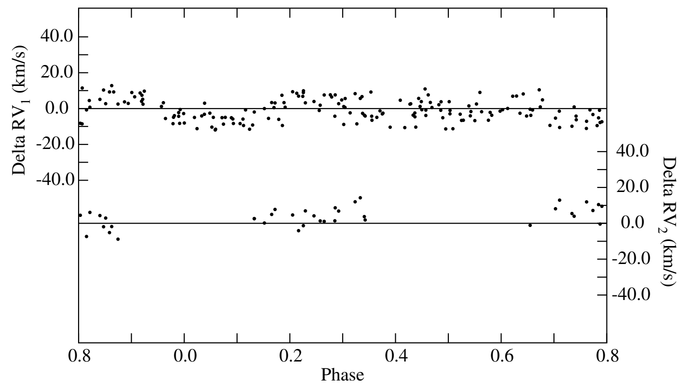

FIG. 6.—Residuals between the theoretical curves and the RV data of Fig. 5.

$R_2 = 1.83 \pm 0.01\ R_\odot$. From the mass, radius, and temperature, the primary component is an A main sequence star. However, the radius for the secondary is too large for a 1 $M_\odot$ main sequence star, and this situation will be discussed in § 8. The WD program provides geometrical information describing the two stars. For overcontact binaries, relative radii are given in three directions: from the center toward the poles, toward the sides, and toward the back (i.e., away from the companion). In addition, it computes "equal-volume" mean radii ($\langle r \rangle$) and the percentage of the Roche lobe ($\langle r \rangle / \langle r \rangle_{\rm lobe}$) that is filled, which is greater than 100% for both components. The contact parameter or fillout factor f (see Van Hamme 1982) is 16%. The radii are listed in Table 8. Figure 7 presents an image of the system at phase 0.75, and the absolute dimensions are provided in Table 9.

From the WD solution, one obtains the bolometric magnitudes (see Table 9) and the individual luminosities as a function of phase, and this information can be used to derive a distance.

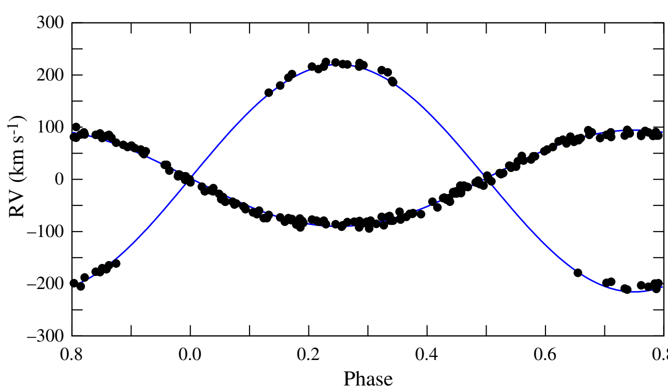

FIG. 5.—Our radial velocities of ES Lib plotted with the Wilson-Devinney solution curves. Zero phase is a time of primary eclipse. See the electronic edition of the *PASP* for a color version of this figure.

The bolometric correction from Flower (1996) for a main sequence star with a temperature of 8500 K is $+0.000$ mag, making $M_V = 0.930 \pm 0.100$ mag. The luminosity ratio at phase 0.25 is 0.103 ± 0.018 in the V bandpass, producing a magnitude difference of 2.468. Thus, the primary is 0.106 ± 0.004 mag fainter than the combined V magnitude. From our data, we determined the system magnitude is 7.259 ± 0.012 mag at phase 0.25. The *Hipparcos* catalog (ESA 1997) listed 7.25 mag but did not provide a phase or an error. Adding the 0.106 and 7.259 mag values, the magnitude for the primary is 7.365 ± 0.013 mag. From the absolute and apparent magnitudes, the computed distance is 194 ± 9 pc. A comparison can be made with the *Hipparcos* data because the listed parallax is $0.0079'' \pm 0.00091''$ (ESA 1997). ES Lib was also included in the "new *Hipparcos* reduction" by van Leeuwen (2007), and he derived $0.00862'' \pm 0.00065''$. These parallaxes correspond to distances of 126.6 ± 14.6 pc and 116.0 ± 8.8 pc, respectively. Our much greater distance may be partially due to the effects of an overly-luminous secondary component and interstellar reddening. From the results of Wolf & Kern (1983), the $b - y$ value of the primary is larger than that expected from its Hβ measurement (Crawford 1979), indicating that there is some interstellar extinction. Gudennavar et al. (2012) produced

TABLE 8
MODEL RELATIVE RADII

Parameter	Value
r_1 (pole)	0.4348 ± 0.0016
r_1 (side)	0.4650 ± 0.0022
r_1 (back)	0.4945 ± 0.0029
$\langle r_1 \rangle$[a]	0.4675 ± 0.0015
$\langle r_1 \rangle / \langle r_1 \rangle_{\rm lobe}$	1.0229 ± 0.0045
r_2 (pole)	0.2936 ± 0.0021
r_2 (side)	0.3072 ± 0.0026
r_2 (back)	0.3450 ± 0.0045
$\langle r_2 \rangle$[a]	0.3185 ± 0.0013
$\langle r_2 \rangle / \langle r_2 \rangle_{\rm lobe}$	1.0370 ± 0.0072

[a] "Equal-volume" mean radii.

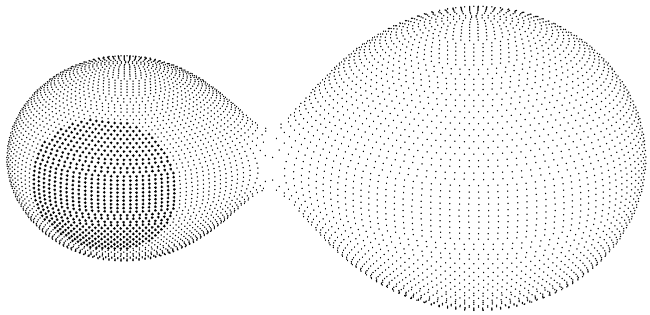

FIG. 7.—Image of ES Lib at phase 0.75. Both stars have overfilled their Roche lobes. The characteristics of the secondary's spot are given in Table 7.

a mean relation between neutral hydrogen column density and color excess. That result, their value of the column density for ES Lib, and the canonical number of 3.3 to convert color excess to total extinction produces $A_V = 0.6$ mag. This value must be increased to 1.1 mag to decrease our distance to the value of van Leeuwen (2007).

6. COMPARISON WITH PREVIOUS RESULTS

The first orbital solution determined for ES Lib was by Bartolini et al. (1973) based on photoelectric V-band measurements and radial velocity observations for the primary. Using the Russell & Merrill (1952) method, they computed two solutions with detached components and a third, possible solution with the primary filling its Roche lobe. Their solutions included a small eccentricity. They determined spectral types of A2–3 V + G3 IV and concluded their best solution gave $M_1 = 2.8\ M_\odot$, $R_1 = 2.5\ R_\odot$, $M_2 = 1.2\ M_\odot$, $R_2 = 1.6\ M_\odot$, $a = 5.5\ R_\odot$, and i in the 60° to 66° range.

Giuricin et al. (1981) reanalyzed the Bartolini et al. (1973) data with the modeling software of Wood (1972). They assumed that $M_1 = 2.6\ M_\odot$ and adopted a mass ratio of 0.4. They computed a single solution with the primary component filling its Roche lobe. They obtained a higher T_1 value of 8900 K and a higher inclination of $73.6° \pm 1.0°$ than we did. Their mass ratio sets $M_2 = 1.04\ M_\odot$, but they had a temperature of 4100 K, placing the detached secondary in the K spectral type range.

Milano et al. (1989) used a "direct search" (i.e., a "grid"-like) method on the Bartolini et al. (1973) data as they obtained solutions with the WD software. They adjusted the inclination, both temperatures, both surface potentials, the mass ratio, and the luminosity of the hotter star. However, they grouped the photometric observations of Bartolini et al. (1973) into normal points. Their final solution found an A3 primary filling its Roche lobe with a detached late-G secondary. Absolute dimensions included $M_1 = 0.98\ M_\odot$, $R_1 = 1.93\ R_\odot$, $T_1 = 7965 \pm 74$ K, $M_2 = 0.55\ M_\odot$, $R_2 = 0.88\ R_\odot$, $T_2 = 4690 \pm 56$ K, $i = 76.34° \pm 0.24°$, and a mass ratio of 0.56. Their results are significantly different from ours.

TABLE 9

FUNDAMENTAL PARAMETERS OF ES LIB

Parameter	Primary	Secondary
$M(M_\odot)$	2.30 ± 0.03	0.97 ± 0.01
$R(R_\odot)$	2.69 ± 0.02	1.83 ± 0.01
$\log g$ (cm s^{-2})	3.94 ± 0.01	3.90 ± 0.01
$M_{\rm bol}$ (mag)	0.93 ± 0.10	3.44 ± 0.19
$L/L_\odot$	33.9 ± 3.2	3.35 ± 0.58

Compared to previous solutions, our solution has at least two distinct advantages. Our data contain over 340 differential magnitudes in each of the UBV bandpasses, and we have radial velocities for both components. Our final results have consistent values for the masses, temperatures, and spectral types, unlike the previous solutions. For example, although the 0.4 mass ratio of Giuricin et al. (1981) is close to our value of 0.423, their $T_2 = 4100$ K is much too low. Likewise, the mass of the primary, $M_1 = 0.98\ M_\odot$, found by Milano et al. (1989) is much too small for an A3 star. We do have a radius for the secondary that is somewhat larger than the main sequence value for a star of that mass and temperature, and this will be discussed in § 8.

We have also analyzed the Bartolini et al. (1973) photometry with the WD software. First, we applied our solution and only allowed the cool spot parameters to vary. The major difference was the longitude position increased by about 20°. The spot's radial size decreased by a couple of degrees, whereas the temperature factor increased by 1%. Then, we solved for the combination of the Bartolini et al. (1973) V photometry and our spectroscopic velocities for all parameters. For this completely independent photometric data set, the overcontact solution, rather than the semidetached configuration, was again preferred. The inclination, surface potential, and mass ratio did not change. Besides some differences in the spot's parameters, the only significant change was a 343 K decrease in the temperature of the secondary. The Bartolini et al. (1973) V photometry has a somewhat smaller standard deviation of 0.008 compared with our V photometry of 0.012. The solution results are listed in Table 10. Figure 8 displays this solution's theoretical curve with the Bartolini et al. (1973) data superimposed, and Figure 9 plots the residuals.

7. VELOCITY SYNCHRONIZATION

From 15 Fairborn Observatory spectra, the rotational broadening fits result in average $v \sin i$ values of 140 ± 5 and 92 ± 4 km s^{-1} for the primary and secondary, respectively. The uncertainties for the projected rotational velocities are conservative estimates. If, as is generally assumed, the rotational and orbital axes are parallel, then the resulting rotational velocities are 149 and 98 km s^{-1} for the primary and secondary, respectively. Adopting our equal volume radii of 2.69 and 1.83 $R_\odot$ produces synchronous rotational velocities of 153.6 and 104.3 km s^{-1}. Thus, the primary is synchronous within its estimated error,

TABLE 10
NEW ANALYSIS OF BARTOLINI ET AL. 1973 PHOTOMETRY

Parameter	Symbol	Solution Values
Period (days)	P	$0.883040881 \pm 0.000000040$
Epoch (HJD)	T_0	$2440712.70830 \pm 0.00034$
Eccentricity	e	0.0[b]
Systemic velocity (km s^{-1})	γ	2.18 ± 0.31
Semimajor axis ($R_\odot$)	a	5.753 ± 0.018
Inclination (deg)	i	70.08 ± 0.16
Mass ratio	M_2/M_1	0.4233 ± 0.0023
Surface potential	Ω_1	2.6842 ± 0.0073
Surface potential	Ω_2	2.6842[c]
Temperature (K)	T_1	8500[b]
Temperature (K)	T_2	5431 ± 42
Luminosity ratio[a]	$L_1/(L_1 + L_2)_V$	0.9265 ± 0.0039
Spot Parameters:		
Latitude (deg)		0.0[b]
Longitude (deg)		297.5 ± 7.9
Radius (deg)		44.5 ± 9.3
Temperature Factor		0.868 ± 0.051

NOTE.—Wilson-Devinney simultaneous solution, including proximity and eclipse effects, of the light and velocity data.
[a] Normalized at phase 0.25.
[b] Adopted value, see text.
[c] Set equal to the surface potential of the primary.

while the secondary is close to synchronous, but its error needs to be 1.5 times larger to include the synchronous value.

8. DISCUSSION

Contact eclipsing binaries named for the prototype variable, W UMa, were divided into two subclasses (Binnendijk 1970) that refer to their light-curve shape. The A-type systems have a transit at primary eclipse, whereas it is an occultation for the W type. From this, it follows that the primary components are hotter than the secondaries in A-type binaries and vice versa for the W types. Thus, although the primary is hotter than the typical W UMa type system (Pribulla et al. 2003), the light curve of ES Lib is that of an A-type W UMa system. More recent work has attempted to subdivide the W UMa systems based on their physical properties (e.g., Maceroni & van't Veer 1996; Csizmadia & Klagyivik 2004).

When thermal equilibrium models for overcontact binaries proved to be unsuccessful, Lucy (1976), Flannery (1976), and Robertson & Eggleton (1977) advanced nonequilibrium models. They postulated that thermal relaxation oscillations occur around a marginal contact state. Thus, a contact binary system would switch between states of good thermal contact (overcontact) and broken contact (semidetached). Robertson & Eggleton (1977) and Lucy & Wilson (1979) predicted that the time in the latter state would be very short.

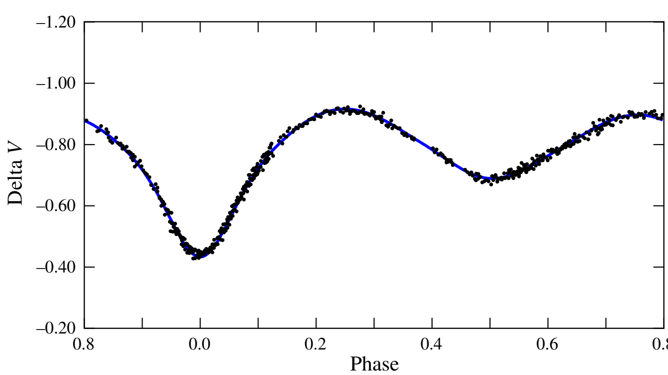

FIG. 8.—Differential V magnitudes of ES Lib obtained by Bartolini et al. (1973) and plotted against the Wilson-Devinney V overcontact solution curve based on their data and our radial velocities. The cool spot, utilized in the solution, moved by about 20°, and the temperature of the secondary is about 340 K cooler, compared to the solution for our data. See the electronic edition of the *PASP* for a color version of this figure.

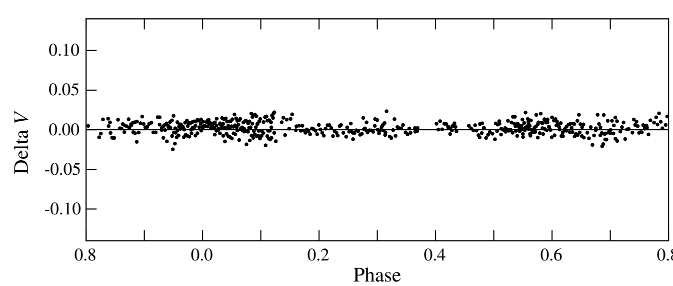

FIG. 9.—Residuals between the theoretical curve and the V data obtained by Bartolini et al. (1973) of Fig. 8.

ES Lib is certainly not a typical W UMa system. The spectral type of the primary is much earlier than traditional W UMa binaries, and thus it could be called an early-type contact system (Kaluzny 1985). An inspection of the contact binary catalog of Pribulla et al. (2003) shows that the orbital period of 0.88304 days for ES Lib is longer than 96% of the 361 W UMa systems that are listed in the catalog. More importantly, the temperatures for each W UMa system indicate that the difference between the two components is relatively small, almost always less than 400 K (Pribulla et al. 2003). This is in stark contrast to the components of ES Lib, which have a difference of over 2700 K. Thus, ES Lib is clearly atypical and appears to be a member of a small group of systems variously called B-type W UMa systems (Lucy & Wilson 1979), systems with contact but with very unequal temperatures (Eggleton 1996), or poor thermal contact systems (Rucinski 1997). These systems have very different eclipse depths but appear to be in contact.

Lucy & Wilson (1979) identified three such possible systems. Shortly thereafter, Kaluzny (1983, 1985, 1986), Hilditch et al. (1984), and Hilditch & King (1988) analyzed additional apparent contact systems that had large temperature differences between the two components. More recently, Siwak et al. (2010) solved light and velocity curves for a dozen systems with components having a large temperature difference, for which at least one previous contact configuration solution was found in the literature. However, Eggleton (1996), Rucinski (1997), and Siwak et al. (2010) have argued that there may be no contact systems with large temperature differences. Rather, the contact solutions are spurious as a result of effects that are not accounted for by the normal Roche lobe geometry, and the systems are instead likely to be semidetached with, at least in a number of cases, accretion hot spots (Siwak et al. 2010).

In the case of ES Lib, the latest version of the WD program, which takes into account a variety of geometries, produces best-fit overcontact solutions to our light curves as well as the V-band data of Bartolini et al. (1973). When we forced the WD program to obtain a barely semidetached solution, the differences between the not-quite overcontact light curve and our adopted overcontact one are modest, but the semidetached solution provides a poorer fit to the observations in several places. While it remains possible that ES Lib is actually in a semidetached configuration, it may require photometric data with a standard deviation as small as 0.001 to resolve the situation. On the other hand, the changing spot distribution, which we have very simply characterized with a single spot in our solutions, may make it impossible to ever clearly differentiate between the semidetached and the best-fit overcontact models.

For ES Lib, because of the overcontact solution with the large temperature difference, we also investigated and obtained a solution using the Mode 6 option in the WD software. This scenario, known as double contact, has both stars exactly filling their Roche lobe. Although an excellent solution was found, the sum of the squares of the residuals was larger for each bandpass than the residuals from the Mode 3 overcontact solution. In addition, we note that for Mode 6 so many constraints have to be met that the double-contact solution is an almost unrealistic situation for binary stars. While there is the possibility this system may fit in the category of a "broken contact" or a "marginal contact" system, similar to that of CN And (Van Hamme et al. 2001) and RU Eri (Williamon et al. 2013), the latter of which has a temperature difference of about 1800 K, the solution of our light and velocity curves of ES Lib clearly prefers the overcontact situation.

There are some significant differences between our results for ES Lib and those of Siwak et al. (2010), who examined a dozen supposed contact binaries with large temperature differences between the components. Unlike many of the systems analyzed by Siwak et al. (2010) as well as some of those examined by Lucy & Wilson (1979), Kaluzny (1986), and Hilditch & King (1988), our light curves of ES Lib show little difference between the heights of the two maxima nor any evidence of third light in the system. In addition, there is no spectroscopic evidence for a hot spot as there are in a number of the systems discussed by Siwak et al. (2010). We also note that many of the very short period binaries examined by Lucy & Wilson (1979), Kaluzny (1985, 1986), and Hilditch & King (1988) did not have mass ratio determinations from radial velocities and needed unphysical values of the albedo of the secondary to produce acceptable light-curve fits. Neither is the case with our data and solution for ES Lib, where we have a well-determined spectroscopic mass ratio, and its light curve can be fitted with the expected albedo and gravitational darkening values. As shown in Figure 1, over the past 40 years the orbital period is constant, so there is no evidence of mass transfer despite the fact that ES Lib is in an overcontact configuration. What ES Lib does share with many of the above analyzed systems is a light-curve solution that, despite the very large temperature difference, results in an overcontact system.

As noted previously, we initially retained two possible overcontact solutions for ES Lib, one with a hot spot on its cool secondary and the second with a cool spot on its secondary. With the primary transferring mass to the secondary, a hot spot might well be expected if the system were semidetached. But the various WD solutions converged to an overcontact situation, and there is no evidence of such a hot spot in our spectra and no significant evidence for additional third light in the system. On the other hand, a cool spot on the star that has a convective outer atmosphere is consistent with the results found for many other overcontact systems (e.g., Strassmeier 1992; Senavci et al. 2011). As a result, we judged the solution with the cool spot on the secondary to be the more likely representation of the system. However, the problem with this solution is how has the system retained the very unequal temperatures of its two components if it is in an overcontact configuration. Perhaps ES Lib has very recently evolved from being a semidetached to an overcontact system, and although the transition to the nearly equal

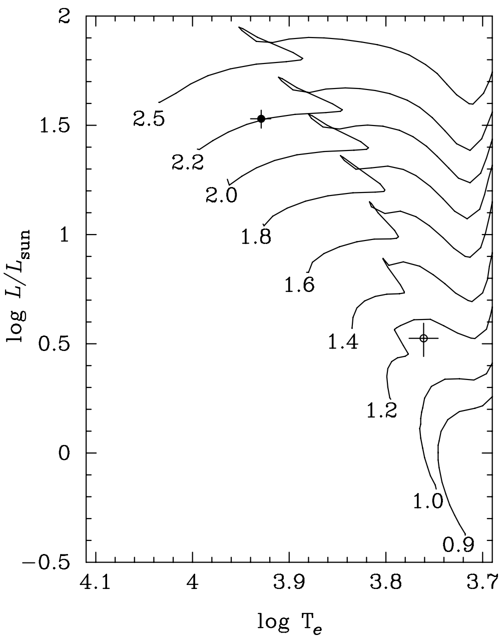

FIG. 10.—Theoretical Hertzsprung-Russell diagram showing the locations of the primary ($M = 2.30\ M_\odot$) and secondary ($M = 0.97\ M_\odot$) of ES Lib compared with the solar-composition evolutionary tracks of Girardi et al. (2000). The mass of each track is labeled in solar masses.

temperatures of a typical W UMa system might be expected to happen quickly, nevertheless, there has been insufficient time for that situation to be reached.

Like other supposed contact binaries with large temperature differences between components, the cooler component of ES Lib is oversized and overluminous for its mass, so there has probably been a past epoch of mass transfer. The radius of the secondary is $1.83 \pm 0.01\ R_\odot$, which is nearly twice that of a main sequence star with $M_2 = 0.97 \pm 0.01\ M_\odot$ and $T_2 = 5774 \pm 57$ K (see Allen 2000). Comparison with the solar abundance evolutionary tracks of Girardi et al. (2000) (see Fig. 10) indicates that the $2.30\ M_\odot$ primary is situated just above the $2.2\ M_\odot$ track, and so its luminosity is approximately correct for its mass. The $0.97\ M_\odot$ secondary, however, has a luminosity that is approximately that of a $1.15\ M_\odot$ star at the end of its main-sequence lifetime.

9. SUMMARY

We obtained new UBV photometric observations and radial velocities for the primary and secondary of the very short-period eclipsing binary ES Lib, which has an orbital period of $0.883040928 \pm 0.000000056$ days. We determined the orbital elements and absolute dimensions with the Wilson-Devinney program. The masses are $M_1 = 2.30 \pm 0.03\ M_\odot$ and $M_2 = 0.97 \pm 0.01\ M_\odot$, while the radii are $R_1 = 2.69 \pm 0.02\ R_\odot$ and $R_2 = 1.83 \pm 0.01\ R_\odot$. Using the results of our WD solution, we compute a distance of 194 ± 9 pc, which is 67% larger than the revised *Hipparcos* value of van Leeuwen (2007). An extinction value of 1.1 mag is required to decrease our distance to that value.

The best simultaneous fits to the radial velocities of the two components and the light curves require that the temperature difference of the two components is over 2700 K and the system is in an overcontact binary configuration rather than semidetached. Two such WD solutions, one with a hot spot on the secondary and the other with a cool spot on the secondary, produce very good fits to the light curves. While both solutions have problems completely explaining the properties of the system, we prefer the cool spot solution.

A comparison with evolutionary tracks indicates that the luminosity of the primary is approximately correct for its mass. However, the secondary appears oversized and overluminous.

This research at Tennessee State University has been supported in part by NSF grant AST-1039522 and the state of Tennessee through its Centers of Excellence program. We thank Walter Van Hamme for valuable discussions about this system and about the WD program's various modes. In addition, he graciously computed the error bars of the parameters in the final solution. The authors thank the anonymous referee for comments, criticisms, and advice that resulted in producing an improved paper. This research made use of the SIMBAD database, operated at CDS, Strasbourg, France.

REFERENCES

Abt, H. A. 2004, ApJS, 155, 175
———. 2009, ApJS, 180, 117
Allen, C. W. 2000, in Allen's Astrophysical Quantities, ed. A. N. Cox (New York: Springer), 388
Barnes, J. R., Lister, T. A., Hilditch, R. W., & Collier Cameron, A. 2004, MNRAS, 348, 1321
Bartolini, C. 1970, Contributi Osservatorio Astronomico di Padova in Asiago, 293
Bartolini, C., Battistini, P., Mammano, A., Margoni, R., & Stagni, R. 1973, Mem. Soc. Astron. Italiana, 44, 231
Bartolini, C., Battistini, P., & Margoni, R. 1968, Inf. Bull. Variable Stars, 290, 1
Batten, A. H., Fletcher, J. M., & MacCarthy, D. G. 1989, Publ. Dom. Astrophys. Obs. Victoria, 17, 1
Binnendijk, L. 1960, AJ, 65, 358
———. 1970, Vistas Astron., 12, 217
Brat, L.et al. 2008, Open European Journal Variable Stars, Czech Republichttp://var.astro.cz/oejv/
B.R.N.O. Project 2011 (Ondřejov: Czech Astronomical Society), http://var2.astro.cz/EN/brno/
Coughlin, J. 2007, undergraduate thesis, Emory Univ
Crawford, D. L. 1979, AJ, 84, 1858
Csizmadia, S., & Klagyivik, P. 2004, A&A, 426, 1001
Diethelm, R. 1990, BBSAG Bulletin, 93, 5

Eaton, J. A., & Williamson, M. H. 2007, PASP, 119, 886
Eggleton, P. P. 1996, in ASP Conf. Ser. 90, The Origins, Evolutions, and Destinies of Binary Stars in Clusters, ed. E. F. Milone, & J.-C. Mermilliod (San Francisco: ASP), 257
ESA 1997, The *Hipparcos* and Tycho Catalogues (ESA SP-1200; Noordwijk: ESA)
Fekel, F. C., Tomkin, J., & Williamson, M. H. 2009, AJ, 137, 3900
Fekel, F. C., Rajabi, S., Muterspaugh, M. W., & Williamson, M. H. 2013, AJ, 145, 111
Flannery, B. P. 1976, ApJ, 205, 217
Flower, P. J. 1996, ApJ, 469, 35
Girardi, L., Bressan, A., Bertelli, G., & Chiosi, C. 2000, A&AS, 141, 371
Giuricin, G., Mardirossian, F., & Ferluga, S. 1981, Astron. Nachr., 302, 187
Gray, R. O., Napier, M. G., & Winkler, L. I. 2001, AJ, 121, 2148
Gudennavar, S. B., Bubbly, S. G., Preethi, K., & Murthy, J. 2012, ApJS, 199, 8
Hardie, R. H. 1962, in Astronomical Techniques, Vol. 2, Stars and Stellar Systems, ed. W. A. Hiltner (Chicago: Univ. Chicago Press), 178
Hendry, P. D., & Mochnacki, S. W. 2000, ApJ, 531, 467
Hilditch, R. W., & King, D. J. 1988, MNRAS, 231, 397
Hilditch, R. W., King, D. J., Hill, G., & Poeckert, R. 1984, MNRAS, 208, 135
Houk, N., & Smith-Moore, M. 1988, Michigan Catalogue of Two-dimensional Spectral Types for the HD Stars, Vol. 4 (Ann Arbor: Univ. Michigan), 249
Johnson, H. L., & Morgan, W. W. 1953, ApJ, 117, 313
Kaluzny, J. 1983, Acta Astron., 33, 345
———. 1985, Acta Astron., 35, 327
———. 1986, PASP, 98, 662
Knigge, R., & Koehler, U. 1969, Veröff. Remeis-Sternw. Bamberg, 8, 83, 10
Krajci, T. 2006, Inf. Bull. Variable Stars, 5690, 1
Lacy, C. H. S., & Fekel, F. C. 2011, AJ, 142, 185
Lucy, L. B. 1967, Z. Astrophys., 65, 89
———. 1976, ApJ, 205, 208
Lucy, L. B., & Wilson, R. E. 1979, ApJ, 231, 502
Maceroni, C., & van't Veer, F. 1996, A&A, 311, 523
Milano, L., Barone, F., Mancuso, S., & Russo, G. 1989, Ap&SS, 153, 273
Nagai, K. 2011, Variable Star Observers League Japan Variable Star Bulletin, 53, 1
Niarchos, P. G., Hoffmann, M., & Duerbeck, H. W. 1997, A&AS, 124, 291
Ogloza, W., Niewiadomski, W., Barnacka, A., Biskup, M., Malek, K., & Sokolowski, M. 2008, Inf. Bull. Var. Stars, 5843, 1
Pribulla, T., Kreiner, J. M., & Tremko, J. 2003, Contrib. Astron. Obs. Skalnaté Pleso, 33, 38
Robertson, J. A., & Eggleton, P. P. 1977, MNRAS, 179, 359
Rossiter, R. A. 1924, ApJ, 60, 15
Rucinski, S. M. 1997, AJ, 113, 1112
Russell, H. N., & Merrill, J. E. 1952, Princeton Obs. Contr., 26, 1
Senavci, H. V., Hussain, G. A. J., O'Neal, D., & Barnes, J. R. 2011, A&A, 529, A 11
Siwak, M., Zola, S., & Koziel-Wierzbowska, D. 2010, Acta Astron., 60, 305
Strassmeier, K.G. 1992, in ASP Conf. Ser. 34, Robotic Telescopes in the 1990s, ed. A. V. Filippenko (San Francisco: ASP), 39
Strohmeier, W. 1966, Inf. Bull. Variable Stars, 164, 1
Strohmeier, W., Knigge, R., & Ott, H. 1964, Inf. Bull. Variable Stars, 62, 1
Scarfe, C. D. 2010, Observatory, 130, 214
Van Hamme, W. 1982, A&A, 105, 389
———. 1993, AJ, 106, 2096
Van Hamme, W., Samec, R. G., Gothard, N. W., Wilson, R. E., Faulkner, D. R., & Branly, R. M. 2001, AJ, 122, 3436
Van Hamme, W., & Wilson, R. E. 1984, A&A, 141, 1
———. 1985, Ap&SS, 110, 169
———. 2007, ApJ, 661, 1129
Van Leeuwen, F. 2007, in Astrophysics and Space Science Library, Vol. 350, *Hipparcos*, The New Reduction of the Raw Data (Dordrecht: Springer)
Williamon, R. M., Sowell, J. R., & Van Hamme, W. 2013, PASP, 125, 17
Wilson, R. E. 1979, ApJ, 234, 1054
———. 1990, ApJ, 356, 613
———. 2012a, J. Astron. Space Sci., 29, 115
———. 2012b, AJ, 144, 73
Wilson, R. E., & Devinney, E. J. 1971, ApJ, 166, 605
Wilson, R. E., Van Hamme, W., & Terrell, D. 2010, ApJ, 723, 1469
Wolf, G. W., & Kern, J. T. 1983, ApJS, 52, 429
Wood, D. B. 1972, A Computer Program for Modeling Non-Spherical Eclipsing Binary Systems (Greenbelt: Goddard Space Flight Center)